

Circuits and Systems for Receiving, Transmitting and Signal Processing

Устройства и системы передачи, приема и обработки сигналов

Research article

DOI: <https://doi.org/10.18721/JCSTCS.18306>

UDC 621.3.049.774.2



DESIGN OF FILTERS USING PSEUDO RESISTORS FOR BIOMEDICAL DEVICES

A.A. Pyatlin  , D.V. Morozov 

Peter the Great St. Petersburg Polytechnic University,
St. Petersburg, Russian Federation

 poccomaxa@cave3d.com

Abstract. The current state of the scientific and technical problem being solved is assessed, initial data are obtained, a 4th-order Sallen–Key filter and a filter with imitation of the inductors by an active circuit based on impedance converters using operational amplifiers and pseudo resistors are developed, and the results are compared. It is recommended to use the low-pass filter with imitation of the inductors in an electronic stethoscope, since it has, compared to the Sallen–Key filter, a less roll-off in the passband, greater attenuation in the stopband, a sharper drop in the frequency response in the transition region, better noise characteristics and a larger dynamic range. The filter with imitation of the inductors has lower nonlinear distortions and demonstrates operability with a spread of temperatures and element ratings, especially in the frequency range containing the main peaks of heartbeat and lung sounds, and the power consumption and hardware costs of such a filter are comparable to similar characteristics of the Sallen–Key filter.

Keywords: electronic stethoscope, Sallen–Key filter, imitation of inductance, pseudo resistor, negative impedance converter, noise characteristic, integrated circuit layout

Acknowledgements: The production of the integrated microcircuit was carried out at the expense of the Ministry of Education and Science of Russia within the framework of the federal project “Training of personnel and scientific foundation for the electronic industry” under the state assignment for the implementation of research work “Development of a methodology for prototyping an electronic component base in domestic microelectronic production based on the MPW service”.

Citation: Pyatlin A.A., Morozov D.V. Design of filters using pseudo resistors for biomedical devices. Computing, Telecommunications and Control, 2025, Vol. 18, No. 3, Pp. 68–79. DOI: 10.18721/JCSTCS.18306



Научная статья

DOI: <https://doi.org/10.18721/JCSTCS.18306>

УДК 621.3.049.774.2



РАЗРАБОТКА ФИЛЬТРОВ С ИСПОЛЬЗОВАНИЕМ ПСЕВДОРЕЗИСТОРОВ ДЛЯ БИМЕДИЦИНСКОГО ОБОРУДОВАНИЯ

А.А. Пятлин  , Д.В. Морозов Санкт-Петербургский политехнический университет Петра Великого,
Санкт-Петербург, Российская Федерация roscomaxa@cave3d.com

Аннотация. Проведена оценка современного состояния решаемой научно-технической проблемы, получены исходные данные, разработаны фильтр Саллена—Ки 4-го порядка и фильтр с имитацией катушек индуктивности активной схемой на основе конверторов импеданса с использованием операционных усилителей и псевдорезисторов, проведено сравнение результатов. В электронном стетоскопе рекомендуется использовать фильтр нижних частот с имитацией катушек индуктивности, т.к. он имеет по сравнению с фильтром Саллена—Ки меньшую неравномерность в полосе пропускания, большее подавление, более резкий спад амплитудно-частотной характеристики в переходной области, лучшую шумовую характеристику и больший динамический диапазон. Фильтр с имитацией катушек индуктивности имеет меньшие нелинейные искажения и показывает работоспособность при разбросе температур и номиналов элементов, особенно в диапазоне частот, содержащих основные пики звуков биения сердца и легких, а потребляемая мощность и аппаратные затраты такого фильтра сравнимы с аналогичными характеристиками фильтра Саллена—Ки.

Ключевые слова: электронный стетоскоп, фильтр Саллена—Ки, имитация индуктивности, псевдорезистор, отрицательный конвертор импеданса, шумовая характеристика, топология интегральной схемы

Финансирование: Изготовление интегральной микросхемы осуществлялось за счет средств Минобрнауки России в рамках федерального проекта «Подготовка кадров и научное обеспечение электронной промышленности» по государственному заданию на выполнение научно-исследовательской работы «Разработка методики прототипирования электронной компонентной базы в отечественном микроэлектронном производстве на основе сервиса МКР».

Для цитирования: Pyatlin A.A., Morozov D.V. Design of filters using pseudo resistors for biomedical devices // Computing, Telecommunications and Control. 2025. Т. 18, № 3. С. 68–79. DOI: 10.18721/JCSTCS.18306

Introduction

It is often necessary to solve the problem of eliminating unwanted noises and to allocate the desired frequency range during signal processing. For this purpose, filters are used. Low-pass filters (LPFs) are used in the portable electronic stethoscope, because the main frequency peaks of the input signals are in the range up to 1 kHz. At the same time, it is necessary to take into account that the electronic stethoscope should be compact, and therefore minimize its sizes.

The chip area reduction can be realized by applying several methods. Firstly, it is necessary to get rid of inductors, because they have rather large dimensions, dissipate a lot of energy, and cause deviations from calculated characteristics. Inductors can be eliminated by replacing them with negative impedance converters (NICs) based on operational amplifiers (OpAmps), which significantly reduces the chip area. That is, ARC filter implementation should be applied to solve this problem.

Secondly, it is necessary to reduce the values of capacitances in the chip, because after replacing the inductors, the size of the chip depends on the size of the capacitors it contains, the area of which is directly proportional to their nominal values.

Thirdly, resistors should be replaced by pseudo resistors. The nominal values and, accordingly, the sizes of resistors increase significantly after reducing the nominal values of the capacitors in the filter. The problem of minimizing the resistor area while maintaining its characteristics can be solved by using the pseudo resistor, which is a special MOS transistor(s) connection circuit. Such a pseudo resistor has linear resistance and small area at the same time.

In [1], the stethoscope has been created that has the input range of heartbeat frequencies from 10 to 500 Hz. The amplitude of the input signal is 35–50 mV, and power supply is 3.7 V. A 2nd-order Sallen–Key filter is used.

In [2], a portable electronic stethoscope with a wireless data transmission module is described. The device is equipped with 2nd-order Sallen–Key filter with the cut-off frequency of 1 kHz.

In [3], an electronic stethoscope is developed, which uses a 4th-order Butterworth bandpass filter. The main heart sound oscillations are in the frequency range of 44 to 54 Hz. The filter has the passband gain of 40 dB and the cut-off frequency of 150 Hz.

The research reported in [4] examines the performance of the 3M Littmann 3200 electronic stethoscope, which amplifies the signal by 24 times and operates in the frequency range from 20 to 2000 Hz, covering the most part of the acoustic energy of respiratory and cardiac tones.

The study [5] deals with the development of an electronic stethoscope using MEMS technology. In this case, it is found that the frequencies of heartbeat tones mainly lie in the range from 20 to 600 Hz.

Authors of [6] analyzed the design of a wireless electronic stethoscope that allows the user to remotely record and transmit listening results. The research shows that the fundamental heart rate ranges between 30 and 70 Hz, while the heart tones and faint noises are distributed between 100 and 1000 Hz. The device uses 2nd-order Butterworth filter with the cut-off frequency of 1 kHz and attenuation of 2 dB at it.

In [7], the use of digital stethoscope for diagnosis of heart disease is discussed. It was found that the basic frequency range of a healthy heartbeat is between 20 and 400 Hz. However, frequencies up to 1 kHz should be considered for a complete analysis of the heart, as they include sounds indicative of heart pathologies.

The basic circuits and applications of pseudo resistors have also been considered, for example, the paper [8] analyzed the design of pseudo resistors to be used in LPFs. The study states that a transistor biased in the weak inversion region can act as a linear resistor in a circuit where the resistance is controlled by the gate voltage of the MOS transistor and can provide very high resistance values including hundreds of mega ohms.

The work [9] describes adjustable pseudo resistors in the design of analog LPFs for implantable biomedical devices. The adjustable pseudo resistors, according to this work, are MOS transistors put into the inversion mode in which large resistance values can be achieved. The resistance is regulated by the transistor gate voltage. The transistors are connected in series to increase the resistance.

In [10], the effect of nonlinearity of pseudo resistors on the performance of biomedical equipment is studied. The work uses a double pseudo resistor switching scheme without a control voltage on the transistor gate.

As can be seen, 4th-order Sallen–Key filter is used most often in the electronic stethoscope, which is a realization of Butterworth approximation. Butterworth approximation has a flat frequency response in the passband. However, we would like to achieve a sharper transition between the passband and the stopband in order to more effectively attenuate signals at frequencies of the stopband. Zolotarev approximation helps to accomplish this task. Although Zolotarev approximation has ripples in the passband in comparison with Butterworth approximation, it is possible to significantly reduce attenuation at the cut-off frequency in comparison with Butterworth approximation. We choose for implementation of Zolotarev approximation an active LPF based on NICs with the cut-off frequency of 1 kHz.

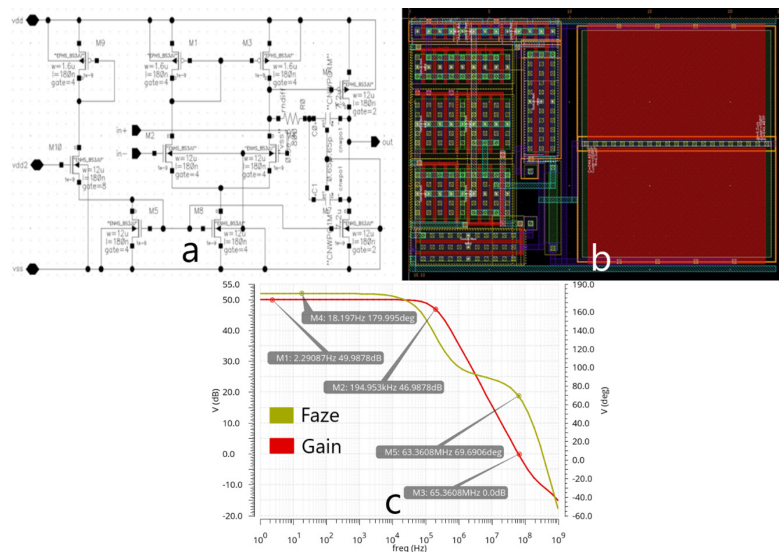


Fig. 1. Schematic (a), layout (b), the amplitude-frequency and the phase-frequency responses (c) of the two-stage OpAmp

Thus, the aim of the work is to design the LPF for the electronic stethoscope. The JSC “Mikron” 180 nm technology is used.

Design of the OpAmp

Firstly, a two-stage OpAmp on MOSFETs was designed, the circuit and layout are shown in Fig. 1a and b. Then a simulation in the frequency domain was conducted, the amplitude-frequency and the phase-frequency responses are shown in Fig. 1c. The OpAmp occupies an area of $345 \mu\text{m}^2$ as shown in Fig. 1b. In addition, the sources and drains of some transistors are united to reduce the chip-on area.

The gain of the OpAmp is 50 dB, the 3dB frequency is 195 kHz and the phase margin is 70° , according to Fig. 1, c. The nonlinear distortion of the OpAmp is 93 dB, and the power consumption is $135 \mu\text{W}$. This characteristic of the OpAmp is obtained at a load of 10 MOhms, which corresponds to the typical loads of the analyzed filters. The characteristics at loads of 5 MOhms, 200 MOhms, 10 pF, 25 pF were also obtained, which correlates with the loads of the filters. These characteristics are sufficiently close to the shown above. This OpAmp is quite simple to implement, but it provides the necessary characteristics and additionally attenuates the signal at high frequencies.

Research of pseudo resistors

Since one of objectives of this work is to minimize the area occupied by the filter, in the proposed filter, first, the large area inductors were replaced by NICs, and then the capacitor values and therefore their area were reduced.

As a result, the resistor nominal values in the filter became large, as well as the area occupied by the resistors. The resistance values of such resistors are to several hundreds of mega ohms. As a result, it is necessary to solve the problem of realization of large resistance values with much smaller on-chip area than ordinary resistors. This problem can be solved by using pseudo resistors in the filter.

A pseudo resistor is a MOS transistor biased to the weak inversion region, which has a near linear and large resistance up to hundreds of mega ohms. However, in this work pseudo resistors based on p- and n-transistors are in saturation. We similarly call these circuits a pseudo resistor because it also provides a linear and large resistance, smaller than transistors in the weak inversion region, but sufficient for the purposes of this work. There are several circuits for connecting MOS transistors into pseudo resistors. For instance, tunable pseudo resistors whose resistance is controlled by the gate voltage, but then each pseudo

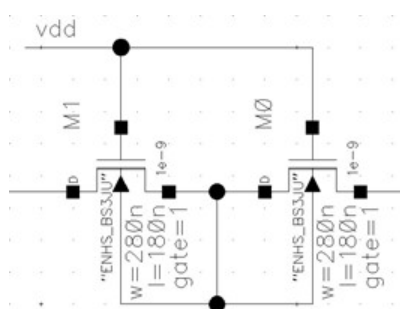


Fig. 2. Pseudo resistor circuit with two transistors

resistor would require a separate voltage source. In this case, it is necessary to create several highly stable voltage sources, which, firstly, is hard, and secondly, requires additional hardware costs and on-chip area.

Therefore, it is much more suitable to include a pseudo resistor with the gate connected to one of the voltage source already used in the filter circuit, thus avoiding the need to create an additional power supply that also consumes additional power. Such a pseudo resistor will have a constant resistance, which can be adjusted by the length and width of the MOS transistor gate. In addition, the resistance value can be increased by connecting several such pseudo resistors in series. Another way to increase the resistance of a pseudo resistor is to use two MOS transistors connected in a certain way, the general circuit of such a pseudo resistor used in the filter is shown in Fig. 2. The transistor substrate is connected to the transistor drain or to the node between the transistors drain and source. Thus, such a pseudo resistor is in a separate area relative to the rest of the chip and has its own potential. Table 1 shows the pseudo resistor resistance depending on the transistor channel length L , the width W and connection type.

Table 1

Resistance of pseudo resistors

$W, \mu\text{m}$	$L, \mu\text{m}$	Resistance of pseudo resistor, kOhm			
		One n-MOS transistor	One p-MOS transistor	Two n-MOS transistors	Two p-MOS transistors
0.28	0.18	21	13	37	23
0.28	1	113	68	195	118
0.28	10	975	747	1700	1270
0.28	100	9600	7460	17000	13200
1	0.18	6.8	4	12	7
10	0.18	0.66	0.36	1.15	0.64
100	0.18	0.065	0.038	0.11	0.064

As we can see from Table 1, the resistance of the pseudo resistor increases with increasing length and decreasing width of the MOS transistor. The two-transistors circuit gives almost twice the resistance of the single transistor. Circuits with n-MOS transistors provide more resistance than those with p-MOS transistors.

Considering the fact that a large resistance has to be realized and creating a separate well for the transistor requires additional area on the chip, two-transistor circuits are chosen for use in the filter. The transistor width is minimum and equals 280 nm and the length is 10 μm , because the properties of the transistor deteriorate if too large a value of the length is taken. To obtain the required resistance

value, such pseudo resistors are placed in series. For instance, in Mikron HCMOS8D technology, the “rndiff” resistor of 1 MOhm has length 5820 μm and width 1.1 μm , and has an area of 6400 μm^2 , while a pseudo resistor with the same value has an area of 130 μm^2 and 25 μm^2 for n- and p-transistors, respectively. The total value of all resistors in the filter with imitation of the inductors is 250 MOhms and it occupies an area of $1.6 \times 10^6 \mu\text{m}^2$, while for pseudo resistors the area would be $2.3 \times 10^4 \mu\text{m}^2$, which reduces the area by a factor of about 70. Similarly, the total value of all resistors in the Sallen–Key filter is 47 MOhms and it occupies an area of $3 \times 10^5 \mu\text{m}^2$, while for pseudo resistors the area would be $6.1 \times 10^2 \mu\text{m}^2$, which reduces the area by a factor of about 50.

Design of 4th-order Sallen–Key filter

The circuit of 4th-order Sallen–Key filter was designed based on [11]. Design of the filter consists in successive complication of the initial circuit and simulation of intermediate filters. Thus, first, a prototype of the filter is assembled, then it is recalculated for the desired frequency, one stage of the Sallen–Key filter is calculated, then two stages using ideal elements. Next, one by one, ideal OpAmps and capacitors are replaced by real ones, and resistors are replaced by pseudo resistors. Calculation of resistor and capacitor values, as well as sequential simulation of the filter circuits are given in [11] as well. Thus, we obtain a filter with real elements, small capacitances in value and area, as well as with pseudo resistors with small sizes and large resistance values. We used the voltage follower based on the OpAmp and the capacitor with capacitance of 10 pF as a load of the filter, because after the filter usually use an analog-to-digital converter (ADC) with this value of input impedance (capacitance) in the electronic stethoscope, and the voltage follower is an element to connect the filter output with the input of the ADC. The supply voltage is 1.8 V, and the input sinusoidal signal with DC value equal to half the supply voltage of 0.9 V is used. The filter cut-off frequency should be 1 kHz, and it is calculated by (1) for one filter stage according to [12]:

$$f = \frac{1}{2\pi\sqrt{R_1 R_2 C_1 C_2}}, \quad (1)$$

where f is the filter cut-off frequency; R_1, R_2 are resistance values; C_1, C_2 are capacitance values.

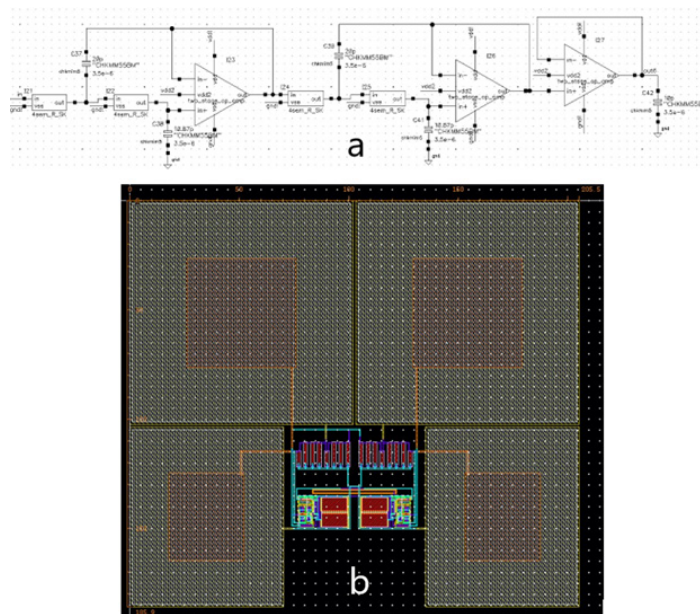


Fig. 3. Circuit (a) and layout (b) of the 4th-order Sallen–Key filter

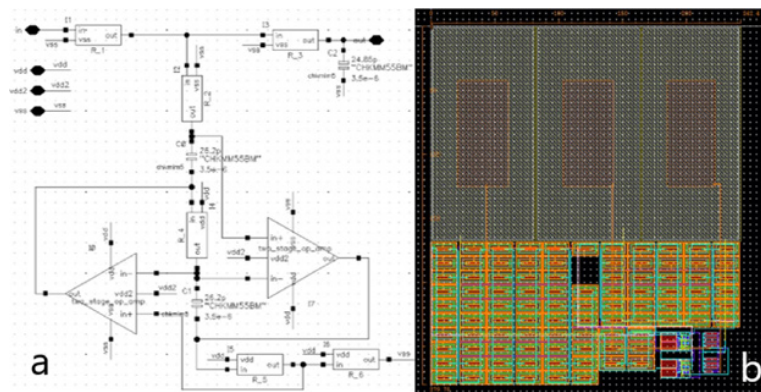


Fig. 4. Circuit (a) and layout (b) of the filter with imitation of the inductors

The final step of design is layout working out and simulation. Fig. 3 shows the circuit and layout of the 4th-order Sallen–Key filter. The area occupied by the filter is 38202 μm^2 . As can be seen from Fig. 3, capacitors take up most of the chip area, however it was possible to significantly reduce the chip area by using pseudo resistors.

Design of the filter with imitation of the inductors

To implement Zolotarev approximation, the filter circuit with imitation of the inductors by an active circuit based on NICs using pseudo resistors is chosen, which allows to achieve less ripples in dB in the passband compared to the monotonic decreasing of the Sallen–Key filter characteristic and greater attenuation. Moreover, it allows to significantly reduce the area occupied by the final filter circuit in comparison with the area of the initial circuit on the chip.

First, a normalized prototype of the 3rd order elliptic filter C0350 is taken from [13]. This filter is then recalculated to the required frequency of 1 kHz, according to the formulas given in [11]. It is possible to replace the inductors with NICs according to [14]. In order to realize the filter with the smallest number of NICs, Bruton transformation of the LCR-prototype should be used, after which a single NIC is required to realize the grounded inductance according to [15]. Therefore, Bruton transformation is applied to the recalculated filter according to the formulas given in [11]. Bruton transformation performs an equivalent transformation of the LCR-circuit of the prototype filter, after which all resistors are replaced by capacitors, inductors – by resistors, and capacitors – by D-elements, supercapacitances. Each supercapacitance, in turn, can be replaced by a single NIC.

Next, similarly to the previous filter, a circuit with ideal elements is created, which, in turn, are replaced by real ones, and resistors are replaced by pseudo resistors. The stages of circuit design, simulation and calculations are given in detail in [16]. It is worth noting that when replacing resistors with pseudo resistors, the choice of the latter with p- or n-MOS transistors depends on the nonlinear distortion they introduce at a given location on the circuit. The circuit and layout of the filter with imitation of the inductors are shown in Fig. 4. The area occupied by the filter is 67819 μm^2 . As can be seen from Fig. 4, with the capacitors occupying more than half of the chip area and the pseudo resistors just under half of the chip area. It was possible to significantly reduce the chip area by using pseudo resistors.

Simulation and comparison of the characteristics of the 4th-order Sallen–Key filter and the filter with imitation of the inductors

Firstly, let us analyze the frequency response of the filters, the simulation of which is shown in Fig. 5.

As can be seen from Fig. 5, the cut-off frequency of both filters is 1 kHz, while ripples in the passband of the filter with imitation of the inductors are less and equal to 0.89 dB, while in the Sallen–Key filter the attenuation is 3 dB. In addition, the filter with imitation of the inductors has more rapid

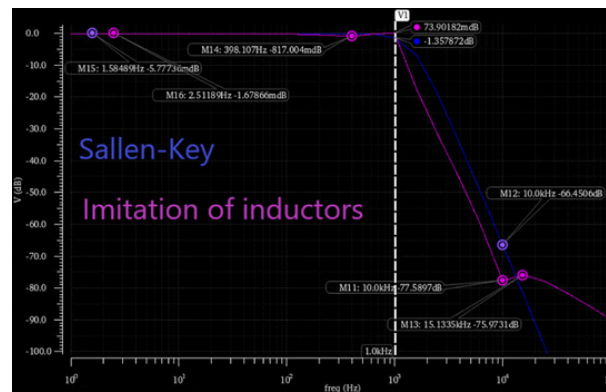


Fig. 5. Frequency responses of Sallen–Key filter and the filter with imitation of the inductors

decline of the frequency response in the transition band, and the stopband starts from 10 kHz with greater attenuation more than 76 dB, while in the Sallen–Key filter attenuation in the stopband is no more than 69 dB. According to these parameters, the filter with imitation of the inductors has some advantages over the Sallen–Key filter.

It is also worth noting that the frequency responses of the filters display the real attenuation of the input signal with the working amplitude. To verify this statement, the simulation in the time domain was performed with the maximum possible amplitude of the input signal of 50 mV and characteristic frequencies of heartbeat and lung sounds, the obtained data were recalculated in dB. As a result, the attenuation values in the time and frequency domains are close.

Next, the filters have been simulated at different temperatures and technology corner parameters. For such simulation, we have considered all possible cases, and then we have selected two worst cases of frequency response up and down relative to the frequency response for typical elements and room temperature. The temperature values are -40 , 27 and 85°C . Since these temperatures allow us to consider the operation of the device at negative temperatures, room temperature as well as at elevated temperatures, this temperature range is much larger than the range of temperatures at which the filter is used. Table 2 shows simulation results of the frequency response of the filters.

Table 2

Comparison of frequency response deviations of the filters

Frequency response type	Cut-off frequency, Hz	Cut-off frequency deviation, Hz	Pass-band ripples, dB	Deviation of the passband ripples, dB	Stopband frequency, Hz	Deviation of the stopband frequency, Hz
Sallen–Key filter						
-40 ss	1636	636	3	0	16873	6873
$+27$ tt	1000	0	3	0	10000	0
$+85$ ff	638	362	3	0	6392	4392
Filter with imitation of the inductors						
-40 ss	1720	720	3	2	22165	12165
$+27$ tt	1000	0	1	0	10000	0
$+85$ ff	500	500	2	1	5100	4900

As can be seen from Table 2, the Sallen–Key filter shows better stability of characteristics when changing temperatures and corner parameters than the filter with imitation of the inductors. However, it should be noted that the ripples of the frequency response of the filter with imitation of the inductors are concentrated at the end of the passband, that is, it does not affect the signals at the characteristic frequencies of heartbeat and lung beats. Moreover, the filter with imitation of the inductors provides more attenuation in the stopband, and the required attenuation is achieved at lower frequencies than for the Sallen–Key filter.

Next, we evaluate the nonlinear distortion of the filters at characteristic heart and lung beat frequencies with the maximum amplitude of the input signal equal to 50 mV. Nonlinear distortions are estimated from the spectrum as the difference of values between the main tone and the next largest harmonics, the results for two filters are given in Table 3.

Table 3

Nonlinear distortions of the filters

Frequency, Hz	50	200	500	800	1000
Nonlinear distortion of the Sallen–Key filter, dB	67	56	53	51	50.9
Nonlinear distortion of filter with imitation of the inductors, dB	70	56	54	50.9	50.2

The nonlinear distortion is slightly less for the Sallen–Key filter at the end of the passband. In addition, it is less for the filter with imitation of the inductors at the start of the passband, where the main peaks of heartbeat sounds are concentrated. At the same time, both filters show acceptable nonlinear distortions, because after the filter it is supposed ADC with $N = 8$ digit capacity, the dynamic range of which is estimated at 49 dB, and therefore nonlinear distortions of the filter should not exceed 49 dB. A larger ADC bit rate is not required, as it is necessary to catch only the main peaks of sounds, but not to get the sound of high quality.

Now let us estimate the dynamic range of the filters. First, we will find the upper limit of the dynamic range. To do this, we will gradually increase the amplitude of the input signal until the nonlinear distortion reaches 49 dB. Thus, we have found the maximum allowable amplitude of the input signal for the Sallen–Key filter equal to 86 mV and for the filter with imitation of the inductors equal to 90 mV. The filter with imitation of the inductors has a slightly larger upper limit of dynamic range.

Then let us consider the noise characteristics of the filters, which are shown in Fig. 6.

The noise response values are smaller for the filter with imitation of the inductors than for the Sallen–Key filter in the whole frequency range except for the end of the passband. The lower limit of the dynamic range of the filters was also determined. The minimum possible amplitude of the input signal for the Sallen–Key filter is 0.6 mV, and for the filter with imitation of the inductors is 0.56 mV.

The dynamic range of the Sallen–Key filter is $20 \log_{10} \left(\frac{86}{0.6} \right) = 43$ dB, and for the filter with imitation of the inductors – $20 \log_{10} \left(\frac{90}{0.56} \right) = 44$ dB. Thus, the dynamic range of the filter with imitation of the inductors is 1 dB larger than the dynamic range of the Sallen–Key filter.

The power consumption of the filters is simulated, which is mainly determined by the power consumption of OpAmps. The power consumption of the filters is similar, since the number of OpAmps in the filters is the same, the power consumption of the Sallen–Key filter is 287 μ W, and that of the filter with imitation of the inductors is 293 μ W.

The areas occupied by the filters on the crystal are also found. For the Sallen–Key filter, the area is 38202 μm^2 , and for the filter with imitation of the inductors it is almost twice as large and equals 67819 μm^2 . Although for the filter with imitation of the inductors the area is larger due to the large

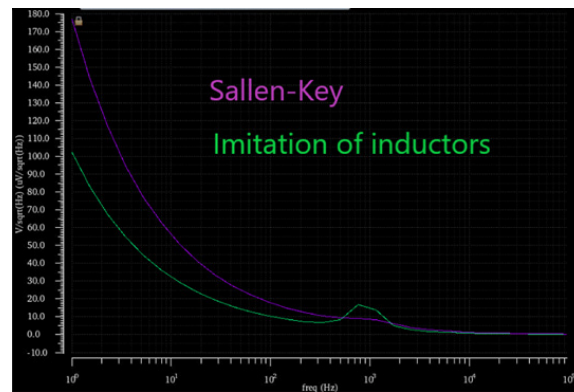


Fig. 6. Noise characteristics of the filters

size of the pseudo resistors, the use of pseudo resistors allowed to significantly reduce the chip area. It should be taken into account that in the electronic stethoscope the ADC is used, the area of which is comparable with filter areas, and the difference in filter areas is not critical in order to be able to make a choice in favor of using the filter with imitation of the inductors in the electronic stethoscope for the rest of the considered characteristics of the filters.

Table 4 summarizes the characteristics of the filter with imitation of the inductors and compares them with similar characteristic of the filters from published works.

Table 4

Characteristics of the filter with imitation of the inductors and the filters from published works

Work	This work	[1]	[17]	[18]	[19]	[20]	[21]	[22]	[22]
Technology, μm	0.18	—	0.35	0.18	0.18	0.18	0.8	0.18	0.18
Filter	II ¹	Bw ²	—	Bq ³	OTA	Bw ²	—	SK ⁴ (rc)	SK ⁴ (sc)
Order	3	4	4	4	9	5	2	2	2
Power supply, V	1.8	9	0.6	1	1.8	1	1.25	—	—
Cut-off frequency, Hz	1000	150	200	500–1000	5400	250	750	610	600
Ripples, dB	0.89	3	1.8	—	—	3.5	—	3	3
Stopband frequency, kHz	10	1	0.6	—	—	1	—	—	—
Attenuation at the stopband frequency, dB	77	40	70	—	—	65	—	—	—
Non-linear distortion, dB	50.2	—	60	40	38	49	49	26	26
Noise, $\mu\text{V}/\sqrt{\text{Hz}}$	8–17	—	—	—	—	20	—	32	21
Dynamic range, dB	44	—	47	55	34	50	62	—	—
Power consumption, μW	293	—	0.9 n ⁵	14 n ⁵	360 n ⁵	450 n ⁵	2.5 n ⁵	413	296
Area, mm^2	0.067	—	0.17	0.13	0.03	0.13	0.23	—	—

¹ Filter with imitation of inductors.

² Butterworth filter.

³ Biquadratic filter.

⁴ Sallen–Key filter.

⁵ Very low power consumption technology has been applied in the development of the filter; the values are given in nW.

Conclusion

The filter with imitation of the inductors by an active circuit based at the NICs with the use of pseudo resistors is proposed for the electronic stethoscope. The problem of area minimization of filters with preservation of their characteristics was solved by successive exclusion of inductors from the filter circuit, reduction of nominal values and areas of capacitances, replacement of resistors by pseudo resistors. The use of pseudo resistors instead of resistors allows to reduce the area occupied by the chip, while keeping the necessary values of resistances.

Mikron 180 nm technology is used. Simulation results for the Sallen–Key filter of the 4th order, as well as for the filter with imitation of the inductors by an active circuit based on the NICs using pseudo resistor were presented based on the filter topologies. Comparison of the filters is carried out and it is revealed that the filter with imitation of the inductors has some advantages over the 4th-order Sallen–Key filter in terms of the obtained characteristics.

Thus, for electronic stethoscope it is recommended to use the LPF with imitation of the inductors, as it provides better or at least the same characteristics as the filters used for the electronic stethoscope in other works.

REFERENCES

1. Waqar M., Inam S., ur Rehman M.A., Ishaq M., Afzal M., Tariq N., Amin F., Qurat-ul-Ain. Arduino based cost-effective design and development of a digital stethoscope. *2019 15th International Conference on Emerging Technologies (ICET)*, 2019, pp. 1–6. DOI: 10.1109/ICET48972.2019.8994674
2. Frank P.-W.L., Meng M.Q.-H. A low cost Bluetooth powered wearable digital stethoscope for cardiac murmur. *2016 IEEE International Conference on Information and Automation (ICIA)*, 2016, pp. 1179–1182. DOI: 10.1109/ICInfA.2016.7831998
3. Malik B., Eya N., Migdadi H., Ngala M.J., Abd-Alhameed R.A., Noras J.M. Design and development of an electronic stethoscope. *2017 Internet Technologies and Applications (ITA)*, 2017, pp. 324–328. DOI: 10.1109/ITECHA.2017.8101963
4. Oliynik V. On potential effectiveness of integration of 3M Littmann 3200 electronic stethoscopes into the third-party diagnostic systems with auscultation signal processing. *2015 IEEE 35th International Conference on Electronics and Nanotechnology (ELNANO)*, 2015, pp. 417–421. DOI: 10.1109/ELNANO.2015.7146923
5. Shi P., Li Y., Zhang W., Zhang G., Cui J., Wang S., Wang B. Design and implementation of bionic MEMS electronic heart sound stethoscope. *IEEE Sensors Journal*, 2022, Vol. 22, no. 2, pp. 1163–1172. DOI: 10.1109/JSEN.2021.3131001
6. Joshi S.S., Patil M.R., Kanawade N.P., More A.P. Bluetooth-based wireless digital stethoscope. *2021 International Conference on Emerging Smart Computing and Informatics (ESCI)*, 2021, pp. 197–202. DOI: 10.1109/ESCI50559.2021.9396835
7. Suseno J.E., Burhanudin M. The signal processing of heart sound from digital stethoscope for identification of heart condition using wavelet transform and neural network. *2017 1st International Conference on Informatics and Computational Sciences (ICICoS)*, 2017, pp. 153–158. DOI: 10.1109/ICICoS.2017.8276354
8. Neshatvar N., Nashash H.A., Basha L.A. Design of low frequency highpass filter using pseudo resistors. *2011 1st Middle East Conference on Biomedical Engineering*, 2011, pp. 407–410. DOI: 10.1109/MECBME.2011.5752152
9. Neshatvar N., Nashash H.A., Basha L.A. Design of low frequency analog low pass filter using tunable pseudo resistors. *2nd Middle East Conference on Biomedical Engineering*, 2014, pp. 39–42. DOI: 10.1109/MECBME.2014.6783202
10. AbuShawish I.Y.I., Mahmoud S.A., Majzoub S., Hussain A.J. Biomedical amplifiers design based on pseudo-resistors: A review. *IEEE Sensors Journal*, 2023, Vol. 23, no. 14, pp. 15225–15238. DOI: 10.1109/JSEN.2023.3280668

11. **Pyatlin A.A.** Chastotno-izbiratel'noe ustroystvo dlia elektretnogo kondensatornogo mikroфона. Vyp. kvalif. rab. [Frequency-selective device for an electret condenser microphone. Final qualifying work], St. Petersburg, 2022, 62 p. DOI: 10.18720/SPBPU/3/2022/vr/vr22-2641
12. **Piatlin A.A., Morozov D.V.** Chastotno-izbiratel'noe ustroystvo dlia elektretnogo kondensatornogo mikroфона [Frequency-selective device for an electret condenser microphone. Final qualifying work]. *Nedelia Nauki IEiT. Materialy Vserossiiskoi konferentsii [Week of Science of the Institute of Economics and Technology. Proceedings of the All-Russian Conference]*, 2022, pp. 112–115.
13. **Zverev A.I.** Handbook of filter synthesis. NY, London, Sydney: John Wiley and Sons, Inc. 1967. 576 p.
14. **Piatlin A.A., Morozov D.V.** Chastotno-izbiratel'noe ustroystvo dlia elektretnogo kondensatornogo mikroфона [Frequency-selective device for an electret condenser microphone. Final qualifying work]. *Nedelia Nauki IEiT. Materialy Vserossiiskoi konferentsii [Week of Science of the Institute of Economics and Technology. Proceedings of the All-Russian Conference]*, 2023, pp. 202–205.
15. **Korotkov A.S.** Switched-capacitor filter designs: tutorial. *St. Petersburg: Polytechnic University Publishing House*, 2014, 191 p. DOI: 10.18720/SPBPU/2/si21-236
16. **Piatlin A.A., Morozov D.V.** Low-pass filter for an electret condenser microphone. *2023 International Conference on Electrical Engineering and Photonics (EExPolytech)*, 2023, pp. 53–56. DOI: 10.1109/EExPolytech58658.2023.10318556
17. **Sawigun C., Thanapitak S.** A 0.9-nW, 101-Hz, and 46.3-μVrms IRN low-pass filter for ECG acquisition using FVF biquads. *IEEE Transactions on Very Large Scale Integration (VLSI) Systems*, 2018, Vol. 26, no. 11, pp. 2290–2298. DOI: 10.1109/TVLSI.2018.2863706
18. **Yang M., Liu J., Xiao Y., Liao H.** 14.4 nW fourth-order bandpass filter for biomedical applications. *Electronics Letters*, 2010, Vol. 46, no. 14, pp. 973–974. DOI: 10.1049/el.2010.1520
19. **Gosselin B., Sawan M., Kerherve E.** Linear-phase delay filters for ultra-low-power signal processing in neural recording implants. *IEEE Transactions on Biomedical Circuits and Systems*, 2010, Vol. 4, no. 3, pp. 171–180. DOI: 10.1109/TBCAS.2010.2045756
20. **Lee S.-Y., Cheng C.-J.** Systematic design and modeling of a OTA-C filter for portable ECG detection. *IEEE Transactions on Biomedical Circuits and Systems*, 2009, Vol. 3, no. 1, pp. 53–64. DOI: 10.1109/TBCAS.2008.2007423
21. **Rodriguez-Villegas E., Yufera A., Rueda A.** A 1.25-V micropower Gm-C filter based on FGMOS transistors operating in weak inversion. *IEEE Journal of Solid-State Circuits*, 2004, Vol. 39, no. 1, pp. 100–111. DOI: 10.1109/JSSC.2003.820848
22. **Chapagai K., Bahubalindrani P., Nishtha.** 2nd Order Sallen Key switched capacitor LPF with N-type transistors. *2018 31st International Conference on VLSI Design and 2018 17th International Conference on Embedded Systems (VLSID)*, 2018, pp. 319–324. DOI: 10.1109/VLSID.2018.83

INFORMATION ABOUT AUTHORS / СВЕДЕНИЯ ОБ АВТОРАХ

Artem A. Pyatlin

Пятлин Артем Андреевич

E-mail: roccomaxa@cave3d.com

Dmitry V. Morozov

Морозов Дмитрий Валерьевич

E-mail: morozov_dv@spbstu.ru

ORCID: <https://orcid.org/0000-0003-3403-0120>

Submitted: 04.10.2024; Approved: 11.09.2025; Accepted: 15.09.2025.

Поступила: 04.10.2024; Одобрена: 11.09.2025; Принята: 15.09.2025.